AFM Tip On-Line Positioning by Using the Landmark in Nano-Manipulation

Shuai Yuan[1-3], Lianqing Liu[1], Zhidong Wang[1,4], Ning Xi[1,5], Yuechao Wang[1], Zaili Dong[1], Zhiyu Wang[1,3]

***Abstract*—AFM has been proved to be a powerful nano-manipulation tool taking advantage of its ultra high resolution and precision. However the large spatial uncertainties associated with AFM tip positioning dual to the PZT nonlinearity and thermal drift are still challenging problems, which hinders its wide application especially in building complex structures In this paper, a probabilistic approach combined with the Kalman filter based localization algorithm is proposed to improve the accuracy of the tip positioning in the task space coordinate frame. A motion model based on the Prandtl-Ishlinskii (PI) model is established, the distribution of model error is statistically obtained through the experimental calibration process. In addition, to further reduce the tip position uncertainties, an environment measurement models is developed through sensing the landmark intermittently with local scanning method during manipulation. Both the simulations results and experimental results are presented to demonstrate the validity of the proposed method.**

I. Introduction

With the rise of nanotechnology, the valuable properties of nano materials and nano devices owing to some specific nanometer-scale elements of their structures has been researched. Their chemical, physical and biological properties depend on the precise nanoscale structures. In order to achieve the desired objectives, the functional elements in complex structures are mainly required to be built manually at the nanoscale. Since AFM was invented with ultra high resolution and precision, and then AFM[1] based manipulation system has been developed to handle the nanoobject. AFM works depending on the interaction force between the tip and the sample surface, and can observe and manipulate the nano-object by ′touching′ it. Hence AFM has been becoming a powerful kernel component to build the nano manipulation system with high performance cost ratio. However there are still some challenging problems in the AFM based manipulation system after more than a decade of its development. In nanomanipulation, AFM tip as the end effector can only apply a point force on the handled object, and can easily slide off it or manipulate it to the wrong place because of the deformation of the cantilever and the tip position error. Therefore the result of each operation has to be verified by a new image scan before next operation starts. This scan-design-manipulation-scan cycle is usually time consuming and inefficient. Since 2004, the AFM based system has been developed with real-time force monitering, and visual feedback based on augmented reality technology with enhancing the reliability of visual feedback through the Kalman filter and local scanning [2-7]. At the same time, the active probe as an end effector is used to avoid deformation of the cantilever that is controlled to be rigid, and maintains its straight shape by applying a control signal to the piezo layer of the cantilever to cancel the cantilever bending caused by the tip-object interaction force. But the errors in the tip positioning in the task space still exist due to the PZT nonlinearity and thermal drift. These spatial uncertainties can hinder the accuracy and efficiency of the AFM based manipulation.

Traditional methods for the PZT nonlinearity and thermal drift are the PZT model and the thermal drift algorithm. The PZT model is divided into three kinds: open loop model based on compensation, closed loop model based on the sensor and composite control model based on the above two methods. Open loop model achieved from Preisach or PI[8, 9] method constructs the feed forward controller and effectively performs dynamics tracking in real-time, but can not reduce the on-line error due to the lackness of feedback. Closed loop model based on the position sensor can get highly reliable and robust compensation effect. But this model can not effectively compensate the positioning error during dynamical tracking and is realized with higher cost. The composite control model can obtain the better effect, but only the positioning error relative to the PZT central-axis can be compensated. The error aroused from thermal drift can not be corrected. Therefore the estimating algorithms such as a Kalman filter and a neural network [10] are proposed for overcome the problems of thermal drift. These methods are based on the compensation model whose effect lies on the degree of the model parameters' accuracy, but it is difficult to obtain the accurate parameters. Recently, a landmark based method is proposed to improve the accuracy of the tip positioning in the task space by sensing the landmark position

This research work is partially supported by National 863 program (Project Code: 2009AA03Z316), the National Natural Science Foundation of China (Project Codes:60904095,60635040) and the CAS/SAFEA International Partnership Program for Creative Research Teams.

1. State Key Laboratory of Robotics, Shenyang Institute of Automation, Chinese Academy of Sciences,Shenyang, 110016, China
2. Shenyang Jianzhu University. Shenyang,110168, China
3. Graduate University of the Chinese Academy of Sciences, Beijing, 100039, China
4. Dept. of Advanced Robotics, Chiba Institute of Technology, Chiba 275-0016, Japan
5. Dept. of Electrical and Computer Engineering, Michigan State University, USA
Contact Author Email: Yuanshuai@sia.cn

that is a feature such as a nanoparticle or a nanorod in the sample surface[2]. During observation of the landmark, the algorithm gets the tip position relative to the center of the nanoparticle by analyzing the scanning line shape of the nanoparticle, and then obtains the tip position in the task space according to the known position of the nanoparticle center. However the tip shape would affect the scanning line geometry[11-13], and increase the spatial uncertainties of the tip position.

In this paper, the PZT nonlinearity and the system thermal drift will be independently considered according to the whole shifting characteristic of thermal drift. Through continuously scanning the sample surface, AFM produces continuous images. The content of these images that render the sample surface are wholly shifting along one direction. According to this experimental phenomena (shown in Section 2), the system thermal drift can be assumed that the sample surface drifts relatively to the tip and there is not the drift during an image scanning or a tip action including a translation or an observation based on local scanning. For the sake of clarity, the tip position will be defined in the image scanning coordinate frame and the task space coordinate frame. The thermal drift will be expressed by the translation of the image scanning coordinate frame in the task space coordinate frame. The two coordinate frames will be coincided by using the same landmark in the sample surface and the thermal drift can be considered as being compensated.

Before nanomanipulation, the sample surface will be first scanned, and this scanning image coordinate frame will be defined as the task space coordinate frame. The landmark such as nanoparticle and nanorod in the sample surface will be identified, and these positions are recorded in the algorithm. During nanomanipulation, a probabilistic approach combined with the Kalman filter by using the landmark is proposed to improve the accuracy of the tip positioning in the image scanning coordinate frame. When the landmark is sensed in the observation, the scanning image coordinate frame will be aligned with the task space coordinate frame according to the position of the landmark. Then the thermal drift is compensated. In the algorithm, the position in the image coordinate frame will be considered as the position in the task space.

As for the spatial uncertainties[14, 15] of the tip position, the probabilistic concept is first used to express the tip position by probability distribution known as probability density function in nano environment. A motion model based on the Prandtl-Ishlinskii (PI) model is established, the distribution of the model error will be obtained by the experimental calibration results. In addition, to further reduce the tip position uncertainties, an environment measurement models is established that the landmark is observed intermittently by the local scanning algorithm during manipulation. Both simulations results and experimental results related to the motion model, the measurement model and the tip position estimation are included to illustrate the validity of the proposed method.

II. Problem Definition

A. The task space coordinate frame and the image scanning coordinate frame

The PZT nonlinearity and the system thermal drift will be independently considered according to the whole shifting characteristic of thermal drift, shown as the following figure.

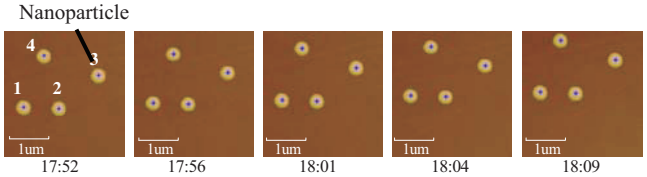

Fig.1. The image shifting due to the thermal drift with the same scanning space.

In the Fig.1, the relative position of the nanoparticle can be considered as not changing according to the relative relationship of the center position of the nanoparticle aligned by the first nanoparticle, as shown in Fig.2.

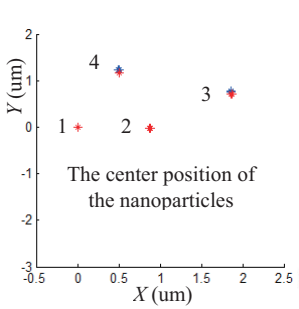

Fig.2. The relative position of the nanoparticle in the shifting image.

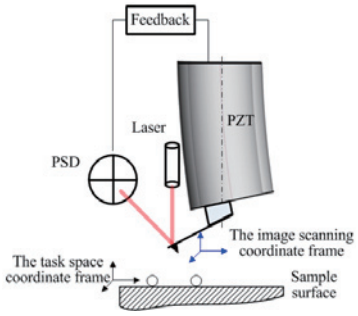

Fig.3. AFM based nanomanipulation system

The first image of the sample surface is defined as the task space coordinate frame. During nanomanipulation, the tip is controlled in the image scanning coordinate frame that is shifting in the task space coordinate frame due to thermal drift, shown as in Fig.3.

B. Compensation principle for the PZT nonlinearity and thermal drift.

1. The PZT nonlinearity will only be considered in the tip action including translation or observation based on local scanning.

2. Thermal drift will be compensated after aligning the task space coordinate frame and the image scanning coordinate frame through observation based on using the landmark.

3. The tip position in the task space coordinate frame will be expressed by the tip position in the image scanning frame. Before each nanomanipulation, the landmark will be observed to coincide the two coordinate frame to improve the accuracy of the tip position.

III. A PROBABILISTIC APPROACH INCORPORATING THE KALMAN FILTER BASED ON OBSERVATION OF THE LANDMARK

The probabilistic approach for AFM tip on-line positioning includes the following three parts: Developing the probability based motion model of AFM tip; Establishing the environment measurement model based on local scanning; Estimating the probabilistic position of the tip by using the Kalman filter method[16].

A. A probabilistic motion model of AFM tip

As for the PZT nonlinearity, the PI model is widely used to build the forward feedback controller to predict the tip position. The PI model is the superimposed result of the basic delay cells, as showed in Fig.4. The formulas from (1) to (8) show the deduced details for PZT nonlinearity compensation by using PI model based method[8, 9]. The compensation results for the PZT compensation are shown as the blue dots in Fig.5.

$$y(t) = H(x(t), y(t_i), r) \tag{1}$$

$$H[x](t) = w^T H_r[x, z_0](t) \tag{2}$$

$$H_r[x, z_0](t)^T = (H_{r_0}[x, z_{00}](t), \cdots, H_{r_n}[x, z_{0n}](t)) \tag{3}$$

Inverse model parameters are calculated as following:

$$H^{-1}[y](t) = w'^T H_{r'}[y, z'_0](t) \tag{4}$$

$$r'_i = \sum_{j=0}^{i} w_j (r_i - r_j) \tag{5}$$

$$w'_0 = \frac{1}{w_0} \tag{6}$$

$$w'_i = \frac{w_i}{(w_0 + \sum_{j=1}^{i} w_j)(w_0 + \sum_{j=1}^{i-1} w_j)} \tag{7}$$

$$z'_{oi} = \sum_{j=0}^{i} w_j z_{0i} + \sum_{j=i+1}^{n} w_j z_{0j} \tag{8}$$

where $i = 1, \cdots, N$ .N is the number of the delay cells.

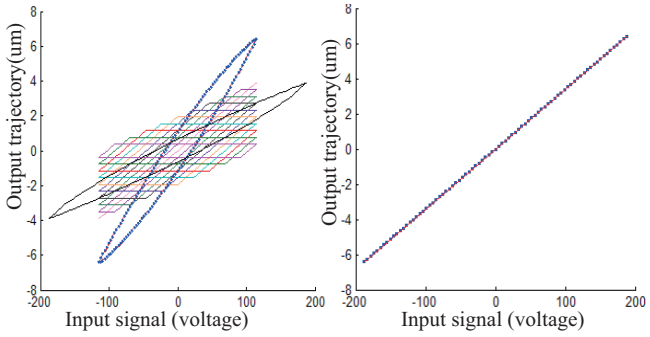

Fig. 4 PI model based on measured hysteretic displacement voltage relation.

The tip's new position at time step k+1 is calculated by using the motion model and the control input U(k), as following:

$$X(k+1) = X(k) + HU(k) + v(k), \quad v(k) \sim N(0, Q(k)) \tag{9}$$

$$X = \begin{pmatrix} x_1 \\ x_2 \end{pmatrix} \begin{matrix} x_1\text{: displacement on } x \text{ direction} \\ x_2\text{: displacement on } y \text{ direction} \end{matrix}$$

$$U = \begin{pmatrix} u_1 \\ u_2 \end{pmatrix} \begin{matrix} u_1\text{: control input on } x \text{ direction} \\ u_2\text{: control input on } y \text{ direction} \end{matrix}$$

H is the PZT driven matrix $\begin{pmatrix} H_h^{-1} & H_v^{-1} \end{pmatrix}^T$ (H_h^{-1} is the PZT driven coefficient on horizontal direction, H_v^{-1} is one on vertical direction), $v(k)$ is a noise disturbance demonstrated to be Gaussian with the variance $Q(k)$. The uniformly-spaced indentation experiments are performed on the CD surface by seven times with different step length on the horizontal direction, Fig.6 shows the indentation results (the dynamic error of the PZT on the horizontal and vertical direction is assumed to be distributed independently and identically). The positioning error in each experiment is proved to obey Gaussian distribution, and the variance grows with the increasing of step length. Fig.7 and Fig.8 show the experimental results.

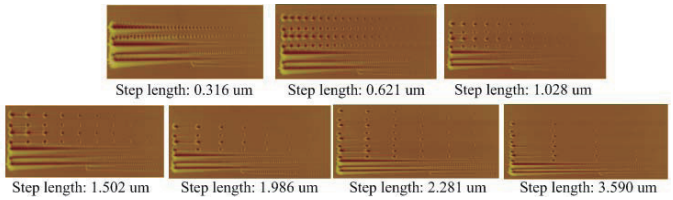

Fig. 6 AFM image of the tip indention at different steps

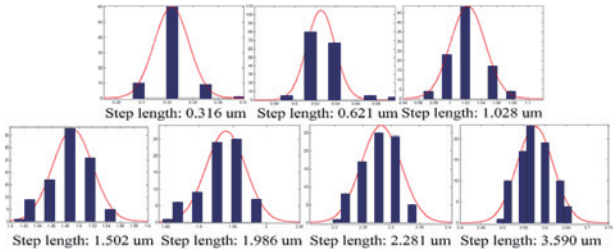

Fig. 7 The error analysis of the tip motion model at different step

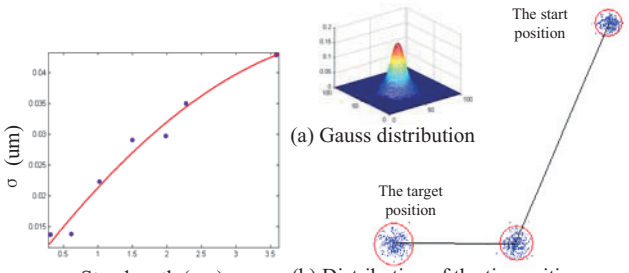

Fig. 8 The variance of the step according with the step length

Fig. 9 Motion model of AFM tip

Fig.9.a shows the noise distribution of the tip motion model. The 2D probabilistic motion model of AFM tip is shown as Fig.9.b that presents how the position uncertainties of the tip grow with the tip motion if no landmark is observed.

B. Establishing the environment measurement model based on local scanning

In the task space, the measurement model of the tip sensing the nanoparticle is shown in Fig.10. Fig.10.b shows the tip is moved from X_s (initial probabilistic distribution P_s) to the landmark X_e (P_e). To localize the tip, the landmark L is locally scanned following the scan pattern shown in Fig.10.a. The scan sequence is scheduled according to the probability distribution of the tip's current position. The tip first scans along line 1. If the landmark is not detected by the first scan line, the second line moves upward or downward till the landmark is detected.

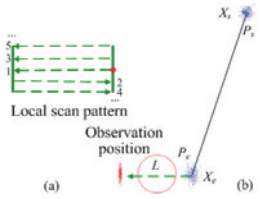

Fig. 10 AFM tip moving path and Observation mode

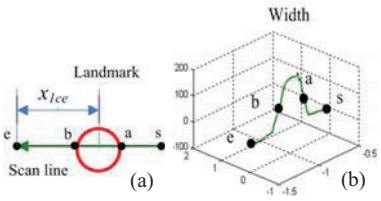

Fig. 11 Observation process and data

If the scan line from point s to point e detects the particle in Fig.11.a, the height information along the scan line should has the shape as shown in Fig.11.b. Assuming that the height of the peak point is greater than r (the radius of the nanoparticle), and the midpoints on both sides of the peak point are b and a, the nanoparticle center x_{lci} on the horizontal direction can be calculated through equation (10), and is assumed contaminated by a zero-mean Gaussian noise disturbance w_{1o} with variance Ψ that rises from the initial calculation error of nanoparticle center determination. The observation value x_{1oe} of the tip in the task space coordinate frame is calculated as (11) and is assumed corrupted by a zero-mean Gaussian noise disturbance w_{1ce} with variance R_1(k) that rises from the tip translation x_{1ce} via the nanoparticle center. Fig.12 is the simulation result, which demonstrates that the tip position accuracy can increase to a certain extent after sensing the landmark.

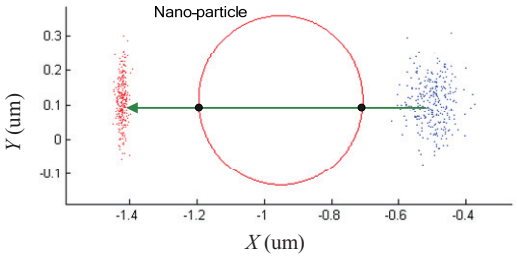

Fig. 12 Distribution of the tip position based on a measurement upon executing a horizontal local scanning motion. The diameter of the nanoparticle as the landmark of the measurement is 200nm.

Observation equations:

$$x_{1lci} = (x_a + x_b)/2 + w_{1o}, \qquad w_{1o} \sim N(0, \Psi) \tag{10}$$

$$x_{1ce} = x_{1e} - x_{1lci}$$

$$x_{1oe} = x_{1lcs} + x_{1ce} + w_{1ce}$$

$$x_{1oe} = x_{1e} + w'_{1ce} \qquad w'_{1ce}(k) \sim N(x_{1lcs} - x_{1lci}, R_1(k)) \tag{11}$$

Through horizontal observation, the tip positioning error can be compensated on the horizontal direction. The same strategy can be applied to the vertical direction as shown in Fig.13. Combined these two directions together, the tip observed position can be calculated through the following equation:

$$z_i(k+1) = x(k+1) + w_{ce}, \quad w_{ce} \sim N(x_{lcs} - x_{lci}, R(k)) \tag{12}$$

where $x(k+1)$ is the vector expressed as:

$$x(k+1) = \begin{pmatrix} x_{1oe} \\ x_{2oe} \end{pmatrix} \begin{matrix} x_{1oe}\text{: the observation value on } x \text{ direction} \\ x_{2oe}\text{: the observation value on } y \text{ direction} \end{matrix}$$

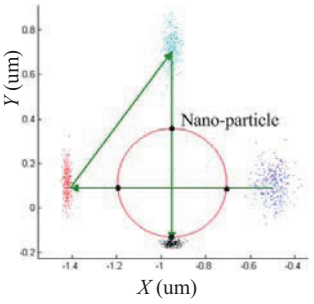

Fig. 13 Distribution of the tip position based on a measurement upon executing a full local scanning motion consisting of a horizontal and a vertical scanning motion respectively.

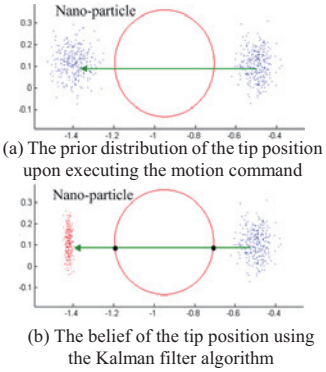

Fig. 14 The prior distribution and belief of the tip position by using the Kalman filter algorithm upon executing a

C. Probabilistic Estimation of the tip position based on Kalman filter algorithm

The tip position $x(k+1|k+1)$ is estimated at time step k+1 based on the prediction of the position $x(k+1|k)$ at time step k (seeing (13)), and the prediction of new observation $z(k+1)$.(seeing(15)). The variance $P(k+1|k)$ is calculated as

Prediction equations:

$$\hat{x}(k+1|k) = \hat{x}(k|k) + Hu(k) \tag{13}$$

$$P(k+1|k) = P(k|k) + Q(k) \tag{14}$$

$$\hat{z}_i(k+1) = \hat{x}(k+1|k) \tag{15}$$

Residual error calculations:

$$v_i(k+1) = [z_i(k+1) - \hat{z}_i(k+1)] \tag{16}$$

$$S_i(k+1) = E[v_i(k+1)v_i^T(k+1)] = P(k+1|k) + R(k+1) + \Psi \tag{17}$$

where $i = 1, 2, \cdots, N$, N is the number of the local scanning.

P: Covariance matrix for state

S: Covariance matrix for sensors

The estimated position $x(k+1|k+1)$ is finally updated based on predictions and observations. The Kalman gain can be calculated as (17). The ∇h^T in the standard result (17) is considered as constant value 1.

$$W(k+1) = P(k+1|k)\nabla h^T S^{-1}(k+1) \tag{18}$$

$$\hat{x}(k+1|k+1) = \hat{x}(k+1|k) + W(k+1)v(k+1) \tag{19}$$

$$P(k+1|k+1) = P(k+1|k) - W(k+1)S(k+1)W^T(k+1) \tag{20}$$

Fig.14.a shows the prediction position of the tip calculated through the motion model, and the estimated the tip position is updated by the Kalman filter based algorithm, as shown in Fig.14.b

IV. Simulation and Experimental Results

In this section, localizing the tip in real time during the translation from x_1 to x_6 is simulated to demonstrate the validity of the proposed approach. As shown in Fig.15(a), the uncertainties of the tip position grow rapidly after direct translation without observing the landmark. The tip position is estimated by local scanning the nanoparticle during the translation as shown in Fig.15(b) The first simulation shows direct translation without observing the landmark leads to a larger uncertainties with the position variance (σ_{x6}: 0.055um, σ_{y6}: 0.056um) in Fig.15(a). The second simulation shows translation with locally scanning the landmark L_3 via x_2, x_3, x_4, x_5, and then move to x_6. When the tip is moved to x_2 from x_1, the variance of the belief is enlarged to (0.046um, 0.061 um). Then after local scanning the landmark (using horizontal observation), the observation variance in horizontal direction is decreased to 0.021um, and the variance of the tip belief is also decreased to (0.021um, 0.061um). Since the variance on vertical direction is larger, the algorithm move the tip from x_4 to x_5 and do one more observation to reduce this variance to (0.027um, 0.017um). Finally, the tip is moved to the target position x_6 with a smaller variance (0.037um, 0.020um) compared with the directed translation one (0.055um, 0.056um).

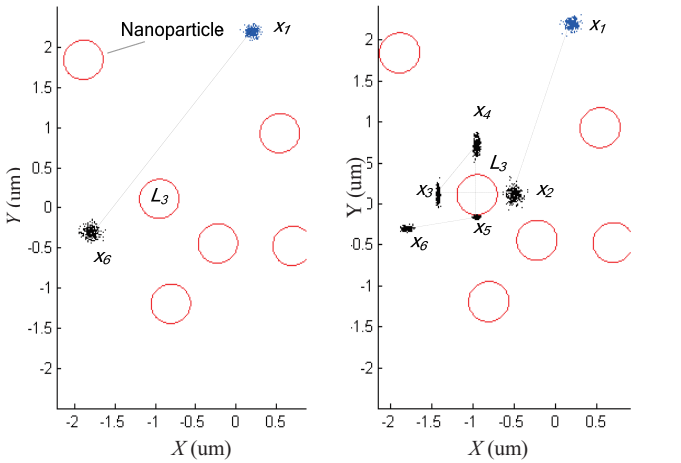

(a) Moving tip directly from x_1 to x_6. (b) Moving tip to x_6 after local scanning

Fig. 15 Distribution of the tip position upon the direct translation and the observable translation between the start position and target position

The experiment results would verify the part of the above simulation results, and include two parts: the results of the measurement model and the results of simple tip positioning.

In the experiments of the measurement model, the nanoparticle as the landmark is first selected or assumed in the scanning image, as shown in Fig.17(c). Second, the tip will be moved to the center of the scanning image; because of the open loop control of the tip translation in X,Y direction, the tip can not be accurately move to the center. So the tip initial position would be estimated by the experiment that moves the tip to the center when the tip is scanning in the first line or last line in the image scanning. The upper bound and lower bound in the vertical direction are obtained, and similarly done in the horizontal direction. Third, according to the tip initial position region, the position of the nanoparticle, the local scanning pattern is designed also in view of the experimental experience, as shown in Fig.16 (b). Fourth, the tip is moved in the light of the scanning pattern, and makes a pit when arriving at the end for demonstration, as shown in Fig.16 (c). Simultaneously, the height information along the tip moving path will be sampled. Last, the design pattern and the experimental results are overlapped to verify the validity of the measurement model.

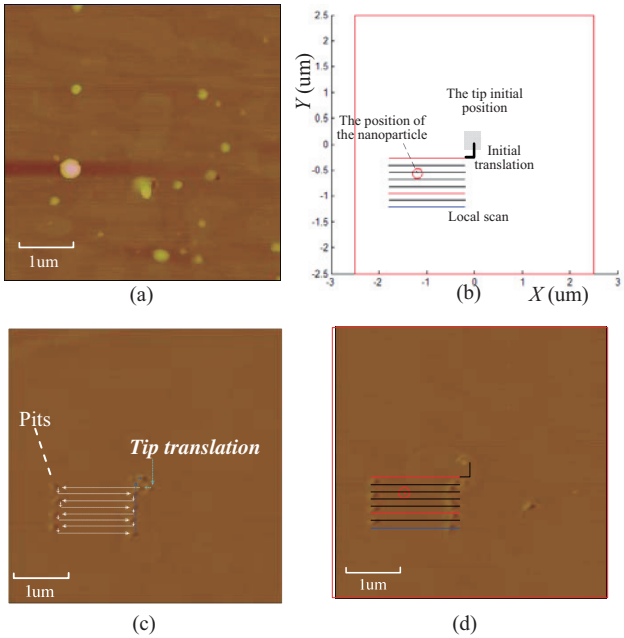

Fig. 18 The experimental results of the environment measurement model based on local scanning. (a) Before nanomanipulation, first image coordinate frame is defined as the task space coordinate frame. (b) Given the position of the nanoparticle, the observation path is designed according to the measurement model. (c) shows the observation procedure based on the local scanning. (d) compares the simulation results with the experimental results.

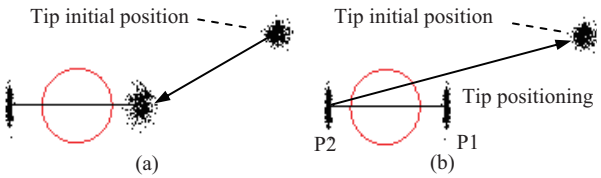

Fig. 17 The design of simple tip positioning. (a) shows that the algorithm moves the tip to the center of the image and then "search" the nanoparticle for tip positioning. (b) presents that the tip is positioned at position P1 and position p2 by sensing the nanoparticle and then go back to the initial position. The spatial uncertainties of tip position at the side of the nanoparticle will be smaller than the one of the center position of the image.

The experimental design of simple tip positioning is shown in Fig.17. The tip is first moved to the center of the image when the manipulation starts. Second, the tip will be positioned by local scanning the nanoparticle based on the

measurement model. When the algorithm has sensed the nanoparticle, the tip will be controlled to accurately make a pit at position P1 and position P2 by sensing the nanoparticle to demo the tip positioning, as shown in Fig.17(b) and Fig.18 (c). Third, the tip will go back to the center of the image, and make a pit. This procedure will be repeated more time. Fig.18 shows that the pits at position P1 and P2 are distributing in the smaller region whose width is about 0.059um(marked by circle 1 and 2 in Fig.18 (b)) than the one whose width is about 1.96um (marked by circle 3). Therefore the experimental results conform to the simulation results. The further experiments are necessary to be performed to obtain the precise error distribution after local scanning the landmark.

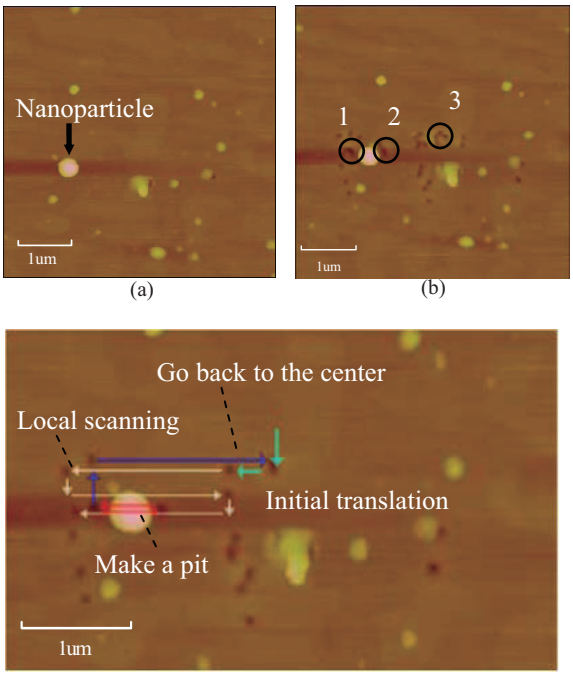

Fig. 18 The experimental results of simple tip positioning. (a) is the failure of local scanning the nanoparticle because of the excessive initial translation in the vertical direction. (b) shows the results of more times of the tip positioning to verify the valid of the algorithm. (c) demonstrates one time of the tip positioning based on local scanning.

V. Conclusions

During nanomanipulation, the tip position relative to the handled object is vital for the manipulated result. Therefore the accuracy of the tip position need to be improved for the high efficiency of nanomanipulation, but it is difficult to archive this objective dual to the PZT nonlinearity and thermal drift. The traditional methods could not effectively reduce the spatial uncertainties of the tip position. In this paper, the PZT nonlinearity and thermal drift are considered independently according to the whole shifting characteristic of the thermal drift and a general framework based on the probability is built by the Kalman filter through sensing the landmark. The tip position is first expressed by the probability distribution in nano environment, and optimally estimated by the kalman filter based on the motion model and the environment measurement model. The simulation for tip positioning is conduct to illustrate that the tip position is updated with smaller uncertainties by the algorithm. The experiment for the motion model, the measurement model, and simple tip positioning also verify the validity of the algorithm despite the fact that some results are inadequate. This method needs to be perfected and confirmed by the experiment in future work.

Acknowledgment

The authors would like to thank Fuqiang Huang of Tsinghua University and Zhiqian Wang of SIA for deducing the algorithm.

References

[1] G. Binning, *et al.*, "Atomic force microscopy," *Phys.Rev.Lett,* vol. 56, pp. 930 - 933, 1986.

[2] L. Lianqing, *et al.*, "Landmark based sensing and positioning in robotic nano manipulation," in *Robotics and Biomimetics, 2008. ROBIO 2008. IEEE International Conference on*, 2008, pp. 37-42.

[3] L. Lianqing, *et al.*, "Sensor Referenced Real-Time Videolization of Atomic Force Microscopy for Nanomanipulations," *Mechatronics, IEEE/ASME Transactions on,* vol. 13, pp. 76-85, 2008.

[4] L. Lianqing, *et al.*, "On-line sensing and display in Atomic Force Microscope based nanorobotic manipulation," in *Advanced intelligent mechatronics, 2007 IEEE/ASME international conference on*, 2007, pp. 1-6.

[5] C. Heping, *et al.*, "CAD-guided automated nanoassembly using atomic force microscopy-based nonrobotics," *Automation Science and Engineering, IEEE Transactions on,* vol. 3, pp. 208-217, 2006.

[6] L. Guangyong, *et al.*, ""Videolized" atomic force microscopy for interactive nanomanipulation and nanoassembly," *Nanotechnology, IEEE Transactions on,* vol. 4, pp. 605-615, 2005.

[7] L. Guangyong, *et al.*, "Development of augmented reality system for AFM-based nanomanipulation," *Mechatronics, IEEE/ASME Transactions on,* vol. 9, pp. 358-365, 2004.

[8] K. Kuhnen and H. Janocha, "Inverse feedforward controller for complex hysteretic nonlinearities in smart-material systems," *Control Intelligence system,* vol. 29, p. 74 ~ 83, 2001.

[9] P. Krejci and K. Kuhnen, "Inverse control of systems with hysteresis and creep," *Control Theory and Applications, IEE Proceedings -,* vol. 148, pp. 185-192, 2001.

[10] B. Mokaberi and A. A. G. Requicha, "Drift compensation for automatic nanomanipulation with scanning probe microscopes," *Automation Science and Engineering, IEEE Transactions on,* vol. 3, pp. 199-207, 2006.

[11] S. Yuan, *et al.*, "Research on the reconstruction of fast and accurate AFM probe model," *Chinese Science Bulletin,* vol. 55, pp. 2750-2754, 2010.

[12] J. S. Villarrubia, "Morphological estimation of tip geometry for scanned probe microscopy," *Surf. Sci,* vol. 321, pp. 287 - 300, 1994.

[13] K.-i. Shiramine, *et al.*, "Tip artifact in atomic force microscopy observations of InAs quantum dots grown in Stranski--Krastanow mode," *Journal of Applied Physics,* vol. 101, p. 5, 2007.

[14] Sebastian Thrun, *et al.*, *Probabilistic Robotics*. London, England: The MIT Press, Cambridge, Massachusetts, 2005.

[15] S. Thrun, "Probabilistic Algorithms in Robotics," *American Association for Artificial Intelligence.,* vol. 21, p. 93 ~ 109, WINTER 2000.

[16] J. J. Leonard and H. F. Durrant-Whyte, "Mobile robot localization by tracking geometric beacons," *Robotics and Automation, IEEE Transactions on,* vol. 7, pp. 376-382, 1991.